

DEVELOPMENT OF AN AGE–FREQUENCY DISTRIBUTION FOR OCEAN QUAHOGS (*ARCTICA ISLANDICA*) ON GEORGES BANK

SARA M. PACE,^{1*} ERIC N. POWELL,¹ ROGER MANN,² M. CHASE LONG²
AND JOHN M. KLINCK³

¹Gulf Coast Research Laboratory, University of Southern Mississippi, 703 East Beach Drive, Ocean Springs, MS 39564; ²Virginia Institute of Marine Science, The College of William and Mary, Route 1208 Greate Road, Gloucester Point, VA 23062-1346; ³Department of Ocean, Earth, and Atmospheric Sciences, Center for Coastal Physical Oceanography, 411 Monarch Way, 3rd Floor, Old Dominion University, Norfolk, VA 23529

ABSTRACT Ocean quahogs [*Arctica islandica* (Linnaeus, 1769)] are the longest-lived, noncolonial animal known today, with a maximum life span exceeding 500 y. Ocean quahogs are a commercially important bivalve, inhabiting the continental shelf of the North Atlantic Basin. Although considerable information exists on the growth and physiology of *A. islandica*, limited information is available regarding recruitment; accordingly, sustainably managing the fishery is a challenge. To investigate long-term recruitment trends, the age of ocean quahogs from Georges Bank which were fully recruited to the commercial fishery (>80 mm shell length) was determined by analysis of annual growth lines in the hinge plate. Ages of animals representing the fully recruited size range were used to develop an age–length key, enabling reconstruction of the population age frequency. The population age frequency showed that the Georges Bank population experienced an increase in recruitment beginning in the late 1890s. Initial settlement, documented by a few ocean quahogs that were much older, occurred much earlier, in the early 1800s. Following the late 1890s increase in recruitment, the population expanded rapidly reaching carrying capacity in 20–30 y. Recruitment was more or less continuous after this expansion, consistent with maintenance of a population at carrying capacity. Unusually large year classes were not observed, nor were significant periods of high recruitment interspersed with periods of low recruitment. The relationship of growth rate with age for the oldest clams was assessed using the time series of yearly growth increments and the resulting relationship fitted to three models (von Bertalanffy, Gompertz, and Tanaka's ALOG curve). The ALOG model was clearly superior because it allows for persistent indeterminate growth at old age, rather than the asymptotic behavior of the other two and because it allows for a rapid change in growth rate at what is presumed to be maturity.

KEY WORDS: ocean quahog, *Arctica islandica*, recruitment, age–frequency distribution, age–length key, Georges Bank, growth model

INTRODUCTION

The ocean quahog (*Arctica islandica*) is a long-lived bivalve mollusc, with a life span exceeding 500 y (Schöne et al. 2005a, Ridgway & Richardson 2011). A pan-boreal species, the ocean quahog is distributed along both coasts of the North Atlantic Basin (Merrill & Ropes 1969, Dahlgren et al. 2000, Begum et al. 2010). In the northwest Atlantic, ocean quahogs range from Cape Hatteras, NC, to St. George's Bay, Newfoundland. On the northeastern side of the basin, they are found along the European coast from the Bay of Cadiz in Spain to Norway, including Iceland, the British Isles, the Faroe and Shetland Islands, and the Baltic, White, and Barents Seas (Merrill & Ropes 1969; for additional documentation of the North Atlantic range, see Brey et al. 1990, Rowell et al. 1990, Ragnarsson & Thórarinsdóttir 2002, Butler et al. 2009). Ocean quahogs grow to a maximum shell length of about 130 mm and attain a life span commonly exceeding 200 y. Current estimates have aged the oldest specimen at 507 y (Butler et al. 2013), possibly making it the longest-lived, noncolonial animal known to science (Wanamaker et al. 2008; see Wisshak et al. 2009, Titschack et al. 2010 for other long-lived examples) and certainly making it the longest-lived noncolonial biomass dominant in the marine world.

Ocean quahogs inhabit sandy, muddy, and gravelly sediments on the continental shelf, and are commonly found at depths of 25–80 m (Morton 2011), tolerating bottom temperatures up to 16°C and a salinity range between 22 and 35 PSU (Schöne 2013). These sediment burrowing suspension feeders feed on phytoplankton and algae at the sediment–water interface via short, inhalant siphons (Winter 1978, Cargnelli et al. 1999a); however, at self-induced, irregular intervals, and during unfavorable environmental conditions such as periods of low oxygen, ocean quahogs burrow even deeper into the sediment typically for 1–7 days, or longer, at which point they close their shells and switch to an anaerobic metabolism (Taylor & Brand 1975, Taylor 1976). The species is notable for its ability to tolerate long periods without oxygen (Oeschger 1990, Philipp & Abele 2010).

The ocean quahog has been a commercially important species in U.S. waters since the fishery began in 1967 (NEFSC 2009). The species supports commercial fisheries throughout much of its range (Gilkinson et al. 2005, Thórarinsdóttir & Jacobson 2005). At the historic start of the ocean quahog fishery in the United States, most fishing effort was off Delmarva and southern New Jersey. By the early 1990s, 40% of the fishing effort shifted north of Delmarva to the south of Long Island. Landings peaked at 22,000 mt in 1992 (NEFSC 2009). In the late 1990s, fishing effort shifted to the southern New England region. Early in the 2000s, the Long Island region became a focus area (NEFSC 2009). Annual ocean quahog landings in

*Corresponding author. E-mail: sara.pace@usm.edu
DOI: 10.2983/035.036.0106

recent years, from 2010 to 2014, have ranged from about 14,000–16,000 mt. The northern shift of the ocean quahog fishery over the past few decades is in part a response to declining catch rates in the Delmarva and New Jersey fishing grounds (NEFSC 2009); however, an additional important driver is the fact that the more valuable surfclam fishery has shifted north in response to increasing bottom water temperatures (Cargnelli et al. 1999b, Weinberg 2005), and many commercial boats fish in both the surfclam and ocean quahog fishery.

The ocean quahog stock is considered to be relatively unproductive. Recruitment events in ocean quahogs appear to be regional and are thought to be infrequent, with recent larger events occurring once or twice every 20–40 y (Lewis et al. 2001, Powell & Mann 2005, Harding et al. 2008, see also Witbaard & Bergman 2003, Thórarinsdóttir & Jacobson 2005). Although recruitment appears to be rare in the context of the fishery, as these animals commonly exceed 200 y in age, recruitment appears to be frequent considering their longevity. Yet as a result of their slow growth, ocean quahogs do not recruit to the fishery for several decades after settlement (NEFSC 2009). Thus, any increase in stock productivity anticipated from fishing down the stock, judged to have been at carrying capacity in 1980 (NEFSC 2009), would likely be delayed due to the time lag between settlement and recruitment to the fishery (Powell & Mann 2005).

Consideration has been given to the challenge of sustainably managing such a long-lived species (Hennen 2015). The possible infrequency of recruitment suggests that ocean quahogs are vulnerable to overexploitation (Thórarinsdóttir & Jacobson 2005). The limited information available on ocean quahog recruitment, even if providing sufficient information on recent recruitment, does not lend any insight on past recruitment events and the potentially daunting time span for rebuilding, should the stock collapse, and the uncertainty of response as the species is fished down from carrying capacity urge precaution if recruitment capacity is truly limited. Improved management of the ocean quahog fishery and increased confidence in the potential of achieving sustainability are dependent on the development of a long-term recruitment index that will provide guidance as to the frequency and significance of recruitment in ocean quahogs over the extended life span of the species.

The objective of this study was to develop information regarding long-term recruitment patterns of ocean quahogs in the Georges Bank region from the age frequency of the living population. To do so, ocean quahogs were collected from Georges Bank and aged by counting annual growth lines using photographs of a cross-section of the hinge plate of each shell. Analysis of the annual growth increments of selected individuals allowed for the assessment of growth rates using three different growth models. Information on age-at-length enabled the development of an age-length key, permitting reconstruction of the population age frequency, which could then be used to evaluate long-term recruitment trends.

MATERIALS AND METHODS

Sample Collection

Samples of ocean quahogs were collected from Georges Bank (40° 43.66' N, 67° 48.32' W) in May 2015 using a hydraulic

dredge deployed from the *F/V Pursuit* and towed for 5 min. The *F/V Pursuit* dredge is nearly 100% selective for clams 80 mm and larger, which is the size range on which this project is focused. Two dredge tows were required to obtain a sufficient sample size; however, the second tow was taken as close as possible to the location of the first so that the same local population was assessed. The two tows were treated as one sample of the local population.

The shell length (anterior–posterior dimension) of each clam was measured (mm). The first 400 clams measured were retained for analysis. An additional 400 clams were retained that exceeded the upper 20th percentile of the size–frequency distribution established by the initial 400 so that samples for ageing contained sufficient numbers of the rarer largest individuals.

Sample Preparation

Clams were shucked and the paired valves dipped in diluted bleach, rinsed in water, and air-dried overnight. Both valves (if intact) of each individual were measured (mm), labeled, and archived. A subset of clams to be aged was haphazardly selected from each 5-mm size interval present in the collection, beginning with the 80 < 85-mm size class. Clams were sectioned along the shell height axis as close to the origin of the umbo as possible using a modified commercial tile saw to expose the hinge region. The sectioned edge was ground and polished using a wet polishing wheel on 400- and 600- μ m sandpaper grit, and then polished with 6- and 1- μ m diamond suspensions on polishing pads.

The hinge region of each clam was photographed using a high-definition Olympus DP73 digital microscope camera using the Olympus cellSens microscope imaging software. This software permits photographs of the hinge region to be captured at a resolution high enough to distinguish annual growth lines without the use of a stain or acetate peel; however, many photographs were needed to produce a single continuous image of the hinge at high magnification. The individual images were stitched together automatically by the imaging software. To estimate the age for each clam, its hinge image was analyzed by annotating each annual growth line using the ObjectJ plugin in the software ImageJ. This plugin also measures the growth increments, the distance between consecutive growth lines, which allowed for the examination of growth rates of selected individuals.

Identification of Annual Growth Lines

The age of 156 ocean quahogs with known shell lengths was estimated from the Georges Bank region. Ocean quahogs deposit distinct annual growth lines along the hinge and along the ventral margin of the shell. The deposition of annual growth lines has been validated through mark–recapture (Murawski et al. 1982) and continuous sampling experiments (Jones 1980), as well as through stable carbon and oxygen isotope analysis (Schöne 2005a, 2005b).

Either of the growth records from the hinge plate or along the ventral margin can be used to determine the age of an individual. A disadvantage in counting growth lines along the entire valve is that many shells are damaged during the collection process and thus do not have fully intact records, and many animals with fully intact shells often exhibit growth anomalies and disturbances which inhibit accurate identification

of annual growth lines. In addition, records in the hinge region can be incomplete, especially in old specimens and those that lived in a harsh environment, because years of abrasion can result in erosion of the oldest growth lines near the umbo. Furthermore, during periods of extended shell closure, anaerobic glycolysis results in the production of acidic metabolites, which can result in partial dissolution of the hinge plate region (Schöne 2013). These processes can eliminate growth lines, resulting in an underestimate of an individual's age. Thus, the hinge was used for the determination of age and growth increment.

One challenge that arises when aging ocean quahogs is that subannual growth lines are visible in addition to annual growth lines, especially in the early years of life. These subannual growth lines are typically less distinct than annual growth lines, but are still clearly visible without the use of a stain or acetate peel. Harding et al. (2008) used a combination of grayscale imaging of the hinge and scanning densitometry of the image to distinguish subannual growth lines of lower intensity from the higher intensity annual growth lines. Based on Harding et al. (2008), subannual growth lines were omitted from the age count. To confirm that the subannual growth lines were consistently excluded, age counts performed by multiple individuals were compared, as were age estimates using the hinge plate and the entire ventral margin of the valve. Growth rates estimated for the first few decades of life, when subannual growth lines commonly occur, agreed with previous analyses by Jones (1980), Harding et al. (2008), and Murawski et al. (1982).

Another challenge encountered when aging ocean quahogs is the presence of closely spaced consecutive growth bands, often referred to as doublets (Butler et al. 2009). Little information is available in the literature regarding the explanation of doublets. Foster et al. (2009) claim that the doublet is generated by a growth check preceding an annual growth band and thus should only be considered a single year. In contrast, Butler et al. (2009) suggest that the doublet is generated by a year of unusually slow growth; thus, each line in a doublet should be counted as a distinct annual growth band. Although ontogenetic growth rates of ocean quahogs vary from one individual to another, overall, a population of ocean quahogs inhabiting the same area should all experience the same general increases and decreases in growth rates due to environmental factors or variations in food supply. To investigate further whether doublets should be counted as a single growth increment or two discrete annual growth increments, the annual growth lines of three randomly selected clams were counted in two different ways: with all doublets treated as a single year and counting each doublet as 2 y. The distance between each annual growth line in each of the aforementioned scenarios was measured and the time series of yearly changes in growth increment compared among the three individuals.

In the test scenario where all doublets were counted as a single annual growth increment, the resulting ages were underestimated considering the sizes of ocean quahogs that were collected. The latter age estimation method also produced a better fit to a general trend of increases and decreases in population growth that is expected throughout the lifetime of the three individual clams, taking into account the uncertainty that exists when identifying annual growth bands in an ocean quahog, which is likely not greater than ± 5 y (Butler et al. 2013). When doublets were treated as two years, the age estimation

along the hinge and the entire ventral margin did not differ by more than ± 3 y, nor did it differ by more than ± 3 y when age counts from the hinge region from multiple readers were compared for the same clam. For these reasons, and in consideration of the recommendation by Butler et al. (2009) that doublets should be treated as discrete annual growth bands, doublets were counted as two discrete years.

Creating the Age–Length Key

The data for Georges Bank are composed of the shell length and age of all aged individuals. An observed population age frequency was generated by applying the probability of finding the observed ages within each 5-mm size class to the complete size frequency of shell lengths measured. To create an age–length key from the sampled individual ages-at-length, the probability of encountering every age within the size range at each site must first be established; however, this is a challenge because the range of ages within any 5-mm size class will be vastly larger than the number of individuals aged unless scores of individuals are aged in each size class. Though technically feasible, the number of aged animals required to meet standard age–length key requirements is prohibitive in practice. Even in relatively data-rich cases, the problem of missing or inadequately sampled lengths or ages within age or length classes can require estimation (e.g., Kimura & Chikani 1987, Harding et al. 2008, Stari et al. 2010).

In the sampled Georges Bank population, as an example, which is composed of animals of 80–115 mm in shell length, ages range from 54 to 198 y. Thus a sample size of about 150 individual clams would only assign an average of approximately one individual per year assuming no duplicates in age. As shown later, the range of ages within a 5-mm size class is a substantive fraction of this entire age range; thus, any probability function established only on the basis of observed ages will likely considerably bias the probability of occurrence of any specific age because it is highly likely that animals are present in the population with ages not found among the subset of animals aged.

As shown later, the distribution of ages within a length class was typically highly skewed and relatively unpredictable from one age class to another. Thus, the problem of missing ages was attacked using an approach that did not require knowledge of the underlying distribution function. Rather, four metrics were defined for each of the sets of measured ages from the 5-mm size classes, namely, the mean age, the variance in age, the mean differential in years between consecutive ages ordered from youngest to oldest, and the variance in the mean differential between consecutive ages. For each 5-mm size class, 1,000 sets of ages were first drawn of the same number as the number of animals aged. These were drawn randomly with replacement from a range of ages established by the youngest and oldest ages in the size class expanded by the average distance between consecutive ordered ages. The observed value of each of the four considered metrics was compared with the distribution of metric values from the 1,000 drawn sets. The probability of the observed value occurring by chance could thereby be established. The 1,000 simulated age groups were then searched to identify individual sets that fell within a 10th percentile of the position of the observed age group for all four metrics. These select age groups were taken as equally valid estimates of the

probability of age within the 5-mm size class. Minimally, 10 such age groups were retrieved and these plus the observed age group were used to construct the probability of age-at-length for each 5-mm size class.

Considering the small sample size in comparison with the age range, a reasonable concern is whether an increased sample size would change the population age–frequency distribution significantly and, as well, whether the simulated expansion of age-at-length data as previously described, provided a realistic probability distribution. To address this matter, 20 additional animals were aged in the 100 < 105-mm size class. This size class was chosen because it had the age distribution least expected to occur by chance based on the four considered metrics. The original set of individuals had ages from 73 to 198 y. Two questions were posed. First, how many of the ages in the new set were not represented in the old set? The expectation is that this number would be large, indicating that the probability of missing ages in the set of animals aged in any 5-mm length class was high, thus requiring application of a method to fill in missing ages. Second, did the second set of ages differ significantly in distribution as measured by the four aforesaid metrics from the first set? The expectation is that the first set was adequate to establish the age distribution function within a 5-mm size class with sufficient accuracy to be used to estimate the age distribution for the age–length key as previously described. A permutation test was used in which 1,000 sets of ages were drawn with replacement from the original set and the second set compared with the distribution obtained thereby (Noreen 1989) to evaluate the probability that the observed mean and variance of ages of the second set could have been obtained from the first. Note that the other two metrics, which depend on the difference between adjacent ages, cannot be tested using a random draw with replacement, because replacement increases the number of zero differences between adjacent ages and thus biases the test. As a consequence, a variant of the aforesaid test was run in which 1,000 sets of ages of a number equivalent to the original set of ages were drawn without replacement from the combined dataset and the second set of ages compared with the distribution obtained to determine if the new set represented a random draw from the total. All four metrics were evaluated using this test. In addition, a population age frequency was also established by generating the estimated ages from all measured shell lengths using the ALOG growth curve (see subsequent section) for comparison with the one generated from the age–length key.

Growth

The measurements of growth increment width, the distance between two consecutive annual growth lines, were recorded for the five oldest clams. Growth increment widths were determined through the annotation of each annual growth line using the ObjectJ plugin, which provides measurements in units of pixels. The total shell length of an individual divided by the cumulative sum of all growth increment widths allowed a conversion of pixels into millimeters. Three growth models (von Bertalanffy, Gompertz, and ALOG) were used to analyze the data. The first two, both frequently evaluated as growth models for shellfish (e.g., McCuaig & Green 1983, Solidoro et al. 2000, Appleyard & DeAlteris 2001, Chintala & Grassle 2001, Urban 2002), were calculated as follows:

$$\text{von Bertalanffy : } L_t = L_\infty(1 - \exp(-K(t - t_0))) \quad (1)$$

and

$$\text{Gompertz : } L_t = L_\infty \exp(-\exp(-K(t - t_0))) \quad (2)$$

where L_t (mm) is the shell length at age t (years), L_∞ is the asymptotic shell length, K is the growth coefficient, and t_0 is the hypothetical age when shell length would be zero. The third growth model,

$$\text{ALOG : } dL_t = \frac{1}{\sqrt{f(t - c)^2 + a}} \quad (3)$$

was developed for species with continuous indeterminate growth (Tanaka 1982, Tanaka 1988). By integrating Eq. (3) over age, the relationship between age and shell length for ocean quahogs was described using the four-parameter ALOG growth model (Eq. 4):

$$L_t = d + \frac{1}{\sqrt{f}} \log \left(2f(t - c) + 2\sqrt{f^2(t - c)^2 + fa} \right) \quad (4)$$

where a is a measure of the maximum growth rate, c is the age at which the growth rate reaches a maximum, d is a parameter that shifts the body size at which growth is maximum, and f is a measure of the rate of change in growth rate (Tanaka 1988). The ALOG curve was fit using a two-stage fitting process, first by fitting the length data to the ALOG length Eq. (4) and then by fitting both the change in length (Eq. 3) and the length (Eq. 4) relationships simultaneously starting from the solution of the length fit.

RESULTS

Growth

Length-at-age was fit with three models; the von Bertalanffy and Gompertz curve fits are shown in Figure 1. Parameter estimates and associated standard errors are shown in Table 1. The observations of growth increment width-at-age and length-at-age also were fit to the ALOG growth curve equation (Fig. 2). Note in Figure 2 that the curve fits both the growth increment relationship and the relationship of length at age. Note also that the latter fit includes both the rapidly ascending early portion of the animal's life and also the extended period at older age of slow but continuous growth. Importantly, the ALOG curve retains a rational ascending limb at old age that cannot be accomplished by the asymptotic von Bertalanffy and Gompertz curves. In addition, the ALOG curve provides rational ages early in life that likewise fail to be accurately fit by the other two growth models. The parameter estimates for the four-parameter ALOG equation are $a = 0.044932$; $c = 2.007$; $d = 92.7737$; and $f = 0.0023936$. The mean and standard deviation of the residuals to the growth increment curve (Fig. 2, left) are -0.0516 ± 0.4172 . The same analysis for the integrated four-parameter expression for age versus length (Fig. 2, right) yields $1.34 \times 10^{-6} \pm 3.731$. Perusal of Figure 2 (right) shows that the individual growth curves are bimodally distributed about the fitted line at old age. Thus, the mean of the residuals tends to be small, whereas the standard deviation tends to be large. The origin of this bimodality remains uncertain, although the possibility that male and female ocean

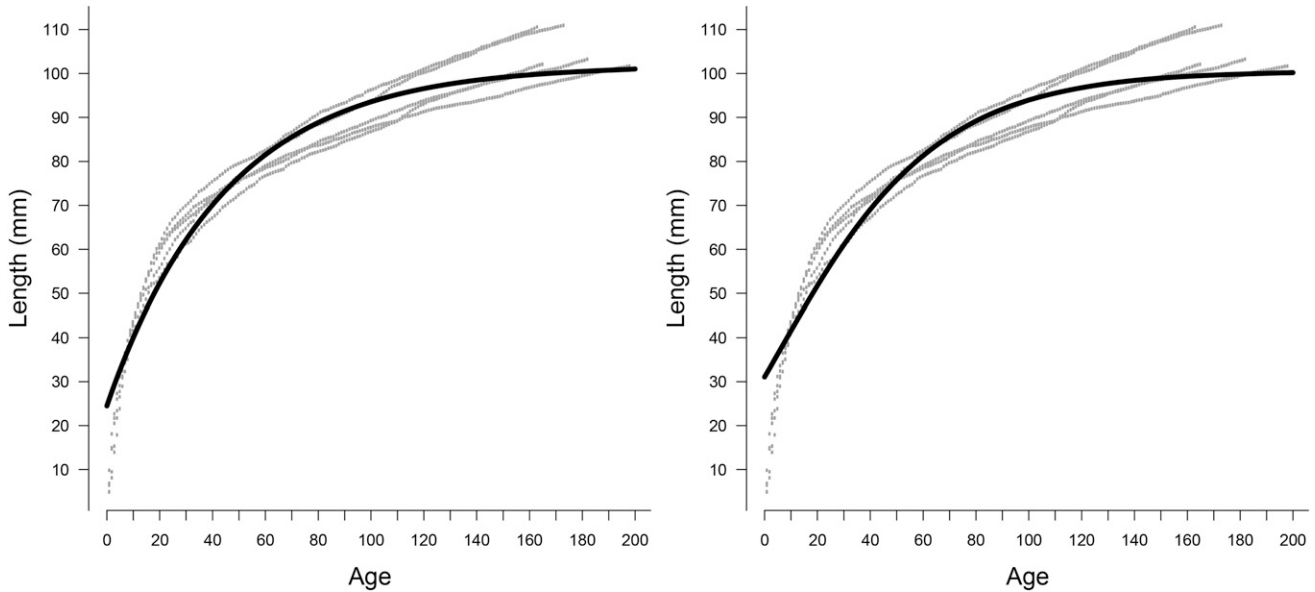


Figure 1. Length-at-age model fits using the von Bertalanffy relationship (left) and Gompertz relationship (right).

quahogs grow at different rates cannot be discounted (Ropes et al. 1984, Steingrímsson & Thórarinsdóttir 1995).

Age Dynamics Within Size Class

The size-frequency distribution from all individuals collected in the two dredge hauls is shown in Figure 3. The shell lengths for 2,780 individuals were recorded. Of these measured clams, 156 individuals greater than or equal to 80 mm in length were aged. Ocean quahogs from this area ranged in age from 54 to 198 y, with animals growing to a maximum length of 116 mm. The observed ages of the sampled animals are shown in Figure 4. These clams have a large age range within each size class (Fig. 5), with the smallest age range of 59 y and the largest age range of 125 y within a 5-mm size class. Similarly, a large variation in size exists at age throughout much of the observed age range (Fig. 4). Thus, the relationship between age and size is highly variable even within narrow age and size categories.

Table 2 shows the statistics for each of the four metrics used to determine if the originally sampled ages were randomly distributed within each size class. Nonrandom test statistics are shaded. The 100 < 105-mm size class is the most nonrandom with three out of four test metrics diverging significantly from random; this is also the size class which had an age range spanning 125 y. The 80 < 85-mm size class was the best behaved, not surprisingly as differential growth rates at age should accrue over time and, thus, should introduce increasingly nonrandom distributions into the larger size classes. Interestingly, it is an intermediate size class that shows the largest deviance from randomness, despite the expectation for the largest size class to be the most nonrandom.

A second group of animals in the 100 < 105-mm size class was aged. Table 3 shows the estimated ages of the original 20 clams and the resampled age estimates for the second set of 20 clams. Eighteen clams in the second set had ages that were not present in the original set of 20 ages. This confirms the expectation that many animals would need to be aged to define the age-length relationship solely from a set of observed lengths and ages.

The statistics listed in Table 2 accordingly were used in the simulation of 10 additional age groups for each size class to identify groups that fell within the shown percentile of the position of the observed age group for all four metrics. The 10 selected simulation groups were used in addition to the observed age group to construct the probability of age-at-length for each 5-mm size class.

Evaluation of Sample Size

A series of permutation tests were run to determine whether the second set of 20 clams aged from the 100 < 105-mm size class were significantly different from the first set. In the first case, the two datasets were directly compared using the observed mean and variance of ages. The two datasets were not significantly different by either metric. In the second group of tests, the likelihood that the second group of ages was a random draw from the combined group was considered. Results indicate that none of the four metrics were significantly different; that is, the second group of ages was a random draw from the combined dataset (Table 4). The lack of statistically significant differences indicates that the age distribution of the first 20 clams sampled does not differ from the second set of 20 clams and suggests that the number of animals aged is sufficient to determine the distribution function for ages within a length class. Additionally, the simulated age groups can be expected to also be representative of that distribution function.

TABLE 1.

Parameter estimates of von Bertalanffy and Gompertz models.

	Von Bertalanffy estimate	Von Bertalanffy standard error	Gompertz estimate	Gompertz standard error
Linf	101.9000	0.4223	100.6000	0.4086
K	0.0225	0.0005	0.0285	0.0007
t ₀	-12.3400	0.6254	5.6510	0.5057

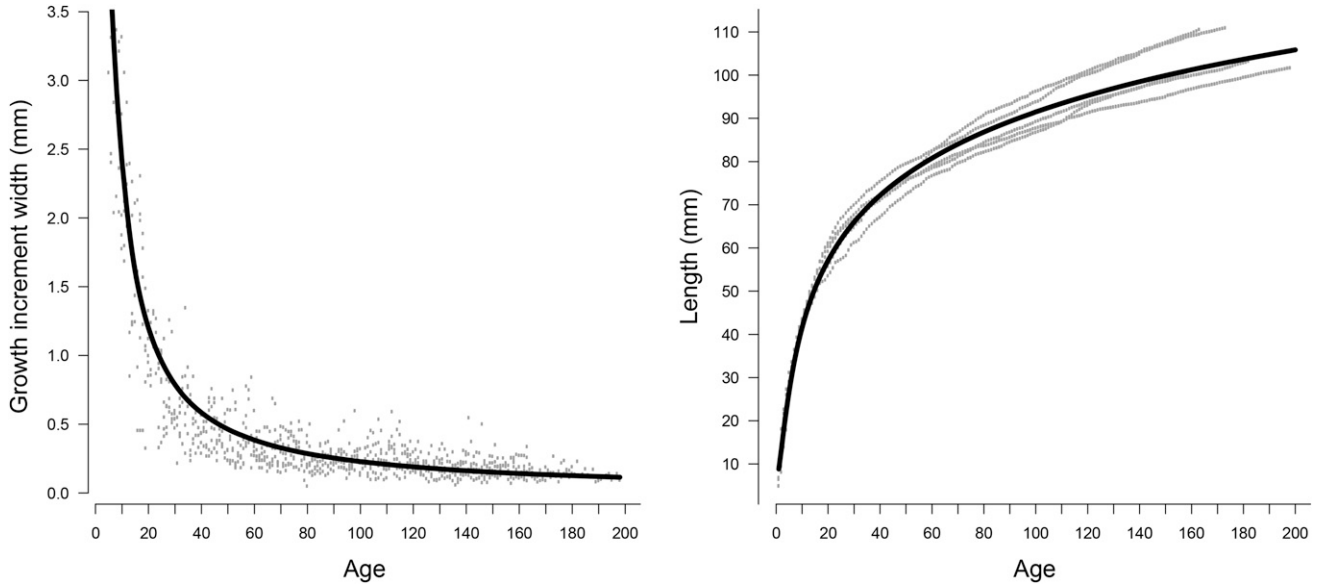


Figure 2. ALOG equation (Eq. 3) fit to age-at-growth increment width (left). Integrated four-parameter ALOG equation (Eq. 4) fit to age-at-length (right).

Age–Length Key

The age–length key (Table 5) was generated by establishing the age probability for each known size class, based on the observed age group plus the 10 simulated groups that were taken as valid estimates of the probability of age within the 5-mm size class. For ease of presentation, the key is shown using 5-mm length classes and decadal age classes. Calculated age frequencies shown subsequently, however, used individual ages rather than a decadal age class. Table 6 shows the estimated number of individuals at age obtained from the two 5-min dredge tows, and was generated by applying the total number of individuals measured (Fig. 3) to the probabilities from the age–length key. Shaded boxes indicate ages with the highest probability of occurring. Table 7 shows the observed age frequency, based only on the 156 sampled ages, which results in many ages being apparently absent from the population.

Earlier analysis of the second set of animals in the 100 < 105-mm size class demonstrates the invalidity of the expectation that this many ages are truly absent. Although the observed and generated age frequencies differ, both show some of the largest numbers of individuals with ages in the late 60’s and between ages 86 and 96 y. The simulated dataset suggests that the peaks of animals at older ages in Table 7 are unlikely, in that many more potential ages exist than could be filled even by one animal given the sample size. Table 6 suggests that the numbers at older ages are more evenly distributed and this expectation is reinforced by Table 3.

Population Age Frequency

The population age–frequency distribution for Georges Bank is shown in Figure 6. This figure was generated from the

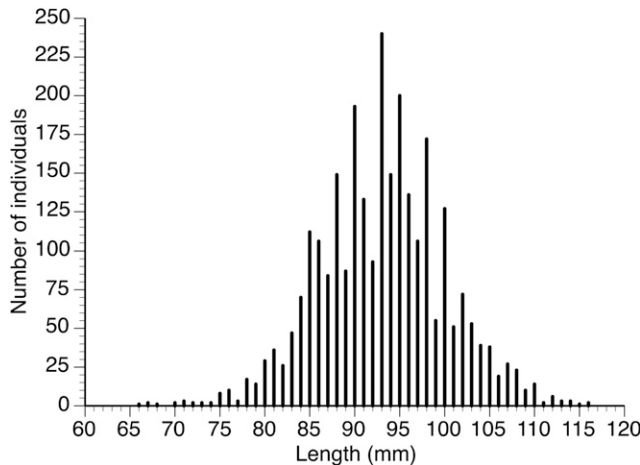


Figure 3. Length–frequency distribution for all animals collected and measured at the Georges Bank site.

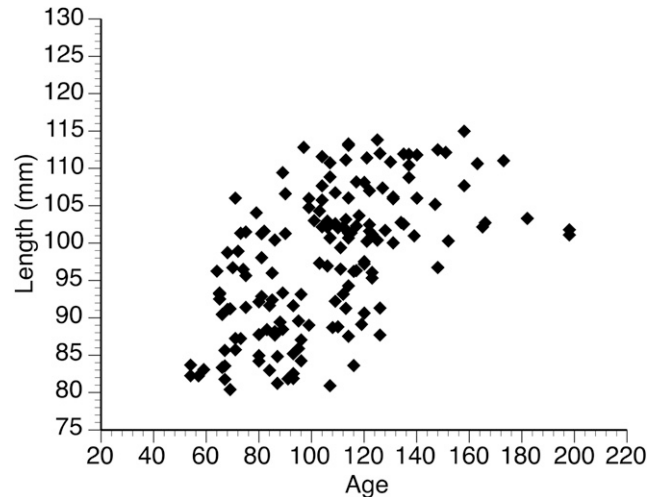


Figure 4. Observed age-at-length of 156 aged ocean quahogs.

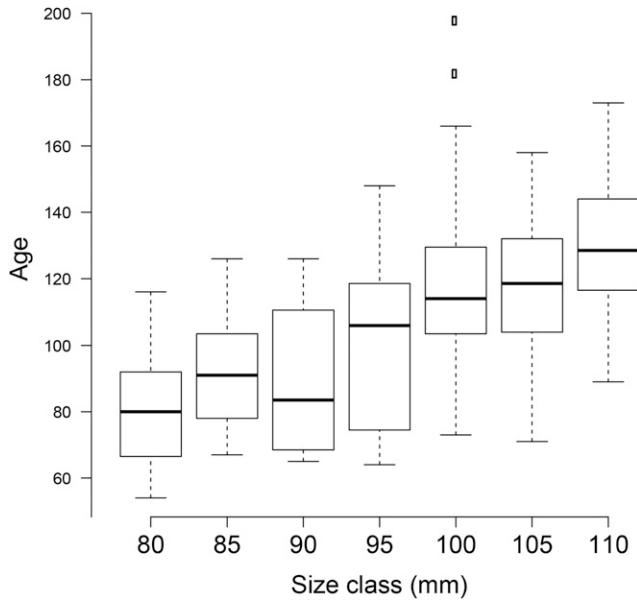


Figure 5. Observed age range within each 5-mm size class. Dark horizontal lines are the medians, boxes show the interquartile range (IQR), error bars represent the full age range excluding outliers (small rectangles) ± 1.5 IQR outside the box.

data in Table 6. The age structure consists of a smattering of animals older than 125 y, a much larger number of animals in the 100- to 125-y age range, and an even larger number of animals in the 65- to 100-y age range (Fig. 6). The population age frequency indicates that ocean quahogs have been present in this region of Georges Bank for about 200 y, since the early 1800s. Given that the oldest animal is substantively younger than the oldest known age for this species and given that the subsampling of the catch included a focus on ageing a subset of the largest animals that averaged modestly older than the smaller individuals (Fig. 5), it is likely that had many animals exceeding 200 y of age been present, at least a few would have been aged. Thus, occupation of this site, although possibly earlier than the birthdate of the oldest animal, was at least very limited in comparison with the age potential of this species.

Assuming that the mortality rate did not vary substantively over the time span represented by the aged animals, the population size remained low for an extended period of time after initial colonization, approximately 70 y, after which the population began to increase in size. This increase began approximately 125 y ago, around the 1890s. Proliferation of the population occurred rapidly over a 5- to 10-y period

TABLE 3. Age data from the original 20 clams sampled and the resample of 20 additional individuals in the 100 < 105-mm size class.

Original ages	Resample ages
73	81
75	82
79	86
99	90
101	104
103	107
106	109
106	113
107	117
110	122
112	122
114	123
114	125
115	128
118	131
121	135
134	139
165	152
182	166
198	198

reaching a stability point around 1900, a relatively short period of time considering the longevity of these animals. The population expansion occurred in two phases with the second phase beginning circa 1915 and approaching a second and higher asymptote circa 1920; thus, over an approximately 30-y period, the population expanded dramatically from a minimal level to its present-day robust population density. After 1920, the population apparently stabilized, with recruitment approximately balancing mortality through the mid-1950s, whereupon the record of measured ages ceases to effectively describe the population age distribution. That is, the decrease in the number of individuals younger than about 65 y is due to the artificial truncation of the dataset at shell length greater than or equal to 80 mm, not to a reduction in recruitment or an increase in mortality. Aging smaller animals would fill out the younger ages, but the problem of age truncation would persist unless animals of all sizes, including young of the year, were aged.

Comparison with ALOG

The population age frequency was also generated using the age estimated from the ALOG curve for each measured length

TABLE 2. Test statistics for each metric in each size class.

	80 mm	85 mm	90 mm	95 mm	100 mm	105 mm	110 mm
Mean	0.1 < P < 0.2	0.1 < P < 0.2	0.05 < P < 0.1	0.1 < P < 0.2	P = 0.005	0.6 < P < 0.7	0.3 < P < 0.4
Variance	0.2 < P < 0.3	0.1 < P < 0.2	0.6 < P < 0.7	0.2 < P < 0.3	P < 0.005	0.05 < P < 0.1	0.05 < P < 0.1
Difference mean	P = 0.4	P = 0.4	P = 0.4	0.4 < P < 0.5	P = 0.4	0.4 < P < 0.5	P = 0.4
Difference variance	0.7 < P < 0.8	0.05 < P < 0.1	0.6 < P < 0.7	0.95 < P < 0.99	0.95 < P < 0.99	0.5 < P < 0.6	0.05 < P < 0.1

Nonrandom statistics are shaded. The difference mean and variance are obtained from the difference between consecutive ages ordered by age.

TABLE 4.
Results of permutation tests comparing the first set of aged animals in the 100 < 105-mm size class to the second.

	With replacement: <i>F</i>	Without replacement: <i>T</i>
Observed mean	<i>P</i> = 0.219	<i>P</i> = 0.320
Observed variance	<i>P</i> = 0.832	<i>P</i> = 0.694
Observed difference mean	–	<i>P</i> = 0.622
Observed difference variance	–	<i>P</i> = 0.657

For the left column, the two datasets were directly compared. Only the first two metrics can be evaluated as any test using a “with replacement” option produces biased results for a set of differences between consecutive ages ordered by age. The second test, using a “without replacement” option investigated the likelihood that the second set of ages represented a random draw from the combined dataset.

(Eq. 4) (Fig. 7). For lengths where the ALOG curve predicted multiple ages, that is, for cases where a 1-mm increase in length covered more than a single year increment in age, the total number of individuals was apportioned evenly over the predicted ages for each length. The age–frequency distribution generated from the ALOG curve can be compared with the previously generated distribution (Fig. 6). Both age–frequency distributions have a similar general shape but differ in substantive ways. In particular, the ALOG approach overpredicts the abundance of old animals and expands the age range well beyond the oldest observed animal. The two distributions differ significantly (Kolmogorov–Smirnov two sample test, $P < 0.05$). Thus, the ALOG curve cannot be used to predict the age structure of the Georges Bank population. Perusal of the age–length key (Table 5) in comparison with Figure 2 showing the ALOG growth model shows that the variability inherent in the population in the age-at-length at large lengths and old ages is primarily responsible for the failure of the growth model to provide sufficient information to generate a population age frequency.

DISCUSSION

Growth

Historically, ocean quahog growth has been modeled using the von Bertalanffy growth curve (e.g., Sager & Sammler 1983, Brey et al. 1990, Steingrímsson & Thórarinsdóttir 1995,

Thórarinsdóttir & Jacobson 2005). The von Bertalanffy growth curve, as well as other growth curves such as the Gompertz curve, lack an inflection point and approach an asymptote (Karkach 2006). The ALOG growth curve (Tanaka 1982, Tanaka 1988) was designed to model an early lag and initial period of exponential growth followed by an indefinite period of continuing albeit perhaps declining indeterminate growth; this type of growth is characteristic of ocean quahogs. The relationship was originally developed for application to the lantern clam *Laternula anatina*, but it has been more widely applied to model the growth of sea urchins (Ebert et al. 1999, Ebert & Southon 2003, Flores et al. 2010). Note that the relationship proves unrealistic for animals where growth asymptotes as it cannot be used to estimate infinite size (Rogers-Bennett et al. 2007)

The ALOG growth curve is the best descriptor of growth in ocean quahogs. This is not surprising considering that the growth of ocean quahogs matches the characteristics of the ALOG growth curve. Growth in ocean quahogs is not asymptotic and, thus, asymptotic growth models often fail to fit growth at old age. Although the von Bertalanffy curve has frequently been used to describe ocean quahog growth in the past, both this curve and the Gompertz curve describe an animal that grows to a maximum size, hence the asymptote that both of these curves approach. Unlike most animals, ocean quahogs have the capacity to live for centuries and continue to grow indefinitely, albeit at a very slow rate.

Moreover, the ALOG growth curve is characterized by a relatively strong change in slope that occurs at an age of approximately 20 y and a size of about 60 mm on Georges Bank. Whether this change in growth rate marks sexual maturity is unknown, but the size demarcation is consistent with the maturity curve presented by Thórarinsdóttir and Jacobson (2005) and Thórarinsdóttir and Steingrímsson (2000), relatively consistent with Ropes et al. (1984), and somewhat larger than inferred from Rowell et al. (1990). Boukal et al. (2014) describe an analogous growth model with similar characteristics dependent on a change in energy allocation at maturity. The metabolic energetics of ocean quahogs beyond the interestingly lower metabolic rate (Begum et al. 2009, Ungvari et al. 2013), the extended capacity for anaerobiosis (Oeschger 1990, Philipp & Abele 2010), and the tolerance to sulfide exposure (Butterworth et al. 2004) are too poorly known to permit a complete metabolic explanation for the growth curve.

The tendency to model the growth of the ocean quahog using asymptotic growth stems from the general agreement of these models with the central more or less two-thirds of the growth

TABLE 5.
Age–length key: probability of each decadal age group occurring within each 5-mm size class.

	50	60	70	80	90	100	110	120	130	140	150	160	170	180	190
80 mm	0.138	0.184	0.161	0.204	0.168	0.066	0.079	0.000	0.000	0.000	0.000	0.000	0.000	0.000	0.000
85 mm	0.000	0.089	0.165	0.231	0.200	0.139	0.100	0.077	0.000	0.000	0.000	0.000	0.000	0.000	0.000
90 mm	0.000	0.238	0.175	0.108	0.150	0.113	0.121	0.096	0.000	0.000	0.000	0.000	0.000	0.000	0.000
95 mm	0.000	0.127	0.140	0.079	0.132	0.233	0.097	0.061	0.040	0.070	0.022	0.000	0.000	0.000	0.000
100 mm	0.000	0.000	0.065	0.085	0.115	0.145	0.180	0.135	0.065	0.075	0.015	0.055	0.025	0.010	0.030
105 mm	0.000	0.013	0.048	0.083	0.075	0.162	0.136	0.167	0.149	0.092	0.061	0.013	0.000	0.000	0.000
110 mm	0.000	0.000	0.000	0.000	0.057	0.077	0.144	0.172	0.191	0.148	0.091	0.077	0.043	0.000	0.000

Zero probabilities indicate the absence of animals at that size and age, given the sampling constraints as discussed in the text.

TABLE 6.

Generated age frequency; number of individuals per tow at each age.

Age	N	Age	N	Age	N	Age	N	Age	N
51	6.86	81	44.99	111	23.57	141	2.43	171	0.03
52	0.00	82	41.51	112	37.53	142	4.31	172	0.03
53	6.86	83	41.10	113	20.95	143	3.39	173	0.72
54	13.71	84	39.30	114	37.18	144	9.40	174	0.03
55	9.14	85	44.16	115	41.83	145	1.93	175	0.03
56	18.28	86	46.41	116	19.21	146	4.81	176	0.00
57	15.99	87	40.20	117	26.94	147	5.11	177	0.00
58	6.86	88	58.17	118	28.91	148	7.79	178	0.00
59	13.71	89	50.44	119	21.28	149	0.44	179	0.00
60	16.56	90	43.72	120	19.04	150	4.83	180	0.00
61	6.86	91	45.63	121	17.08	151	2.43	181	0.00
62	18.90	92	32.23	122	25.29	152	2.67	182	0.66
63	32.48	93	74.74	123	38.60	153	0.91	183	0.00
64	31.01	94	38.94	124	19.22	154	1.71	184	0.00
65	47.49	95	44.78	125	11.54	155	0.74	185	0.00
66	54.46	96	38.97	126	20.53	156	0.91	186	0.00
67	58.84	97	29.74	127	9.15	157	1.52	187	0.00
68	43.92	98	43.19	128	9.19	158	0.44	188	0.00
69	45.15	99	28.57	129	0.91	159	1.66	189	0.00
70	35.39	100	26.44	130	2.36	160	1.03	190	0.00
71	61.24	101	20.67	131	2.52	161	0.88	191	0.00
72	24.99	102	37.16	132	0.61	162	0.17	192	0.00
73	32.99	103	40.78	133	6.66	163	0.13	193	1.33
74	51.51	104	21.04	134	2.73	164	0.00	194	1.33
75	31.10	105	18.99	135	2.24	165	0.74	195	1.33
76	36.93	106	18.76	136	3.79	166	0.69	196	1.33
77	49.56	107	30.58	137	4.97	167	1.35	197	0.66
78	42.21	108	35.73	138	5.13	168	0.00	198	0.66
79	26.22	109	42.49	139	5.52	169	0.08	199	0.66
80	53.36	110	24.53	140	1.91	170	0.74	200	0.00

Shaded boxes represent ages with the highest probability of occurring.

TABLE 7.

Observed age frequency; number of individuals per tow at each age.

Age	N	Age	N	Age	N	Age	N	Age	N
51	0.00	81	56.99	111	37.68	141	0.00	171	0.00
52	0.00	82	0.00	112	45.45	142	0.00	172	0.00
53	0.00	83	37.30	113	38.47	143	0.00	173	0.32
54	54.84	84	65.57	114	92.52	144	0.00	174	0.00
55	0.00	85	56.99	115	7.30	145	0.00	175	0.00
56	0.00	86	74.60	116	46.26	146	0.00	176	0.00
57	27.42	87	54.84	117	20.68	147	1.84	177	0.00
58	0.00	88	37.30	118	7.30	148	19.16	178	0.00
59	27.42	89	77.29	119	37.30	149	0.00	179	0.00
60	0.00	90	1.84	120	77.68	150	0.00	180	0.00
61	0.00	91	27.42	121	7.62	151	0.32	181	0.00
62	0.00	92	0.00	122	1.84	152	0.00	182	7.30
63	0.00	93	130.29	123	37.68	153	0.00	183	0.00
64	18.84	94	0.00	124	0.00	154	0.00	184	0.00
65	114.45	95	74.60	125	0.32	155	0.00	185	0.00
66	65.57	96	102.87	126	75.77	156	0.00	186	0.00
67	92.14	97	0.32	127	1.84	157	0.00	187	0.00
68	56.99	98	0.00	128	0.00	158	2.16	188	0.00
69	65.57	99	46.44	129	0.00	159	0.00	189	0.00
70	18.84	100	0.00	130	0.32	160	0.00	190	0.00
71	76.44	101	7.30	131	3.68	161	0.00	191	0.00
72	18.84	102	0.00	132	0.00	162	0.00	192	0.00
73	44.60	103	26.14	133	0.00	163	0.32	193	0.00
74	18.84	104	4.00	134	7.30	164	0.00	194	0.00
75	64.29	105	0.00	135	0.32	165	7.30	195	0.00
76	0.00	106	33.44	136	0.00	166	0.00	196	0.00
77	0.00	107	36.88	137	2.47	167	0.00	197	0.00
78	0.00	108	37.30	138	0.00	168	0.00	198	7.30
79	7.30	109	39.99	139	0.00	169	0.00	199	0.00
80	130.29	110	44.60	140	2.16	170	0.00	200	0.00

trajectory; however, neither the von Bertalanffy nor Gompertz curve can capture the exponential growth exhibited by juvenile ocean quahogs unlike the ALOG curve nor can they capture the continual growth at old age (e.g., Steingrímsson & Þórarinsdóttir 1995, Ridgway et al. 2012).

Age–Length Key and Generation of a Population Age Frequency

The 100 < 105-mm size class had the most unusual age distribution, spanning an age range of 125 y. This size class also had the most nonrandom distribution with three out of four statistically significant test metrics. Based on these considerations, the 100 < 105-mm size class was chosen to sample an additional 20 clams to determine if the age distribution of the 20 resampled clams significantly differed from that of the 20 original ages. A series of permutation tests revealed no significant differences between the two groups of aged animals in the four metrics chosen to evaluate the age distribution within a 5-mm size class. This suggests that a sample size of 20 individuals per 5-mm class is sufficient to represent the dispersion of ages present in that size class, although not sufficient to represent all ages likely to be present. Given this result for the size class with the most irregular age distribution, encompassing a range of 125 y within a single 5-mm class, a reasonable assumption follows that the other size classes with a sample size of 20 individuals

comprising smaller age ranges with less extreme age distributions are also representative of their respective age distributions.

The number of new ages in a second set of 20, however, confirms the expectation that a large number of aged animals per size class would be required to directly assess the probability of age at size within a size class. Many ages present in the 5-mm size class are not identified in a single sample of 20 individuals. Thus, obtaining a representative age–length key requires assumptions of the underlying age distribution function within a size class, unless one is prepared to age many hundreds of clams. Two options were compared. In one case, ages were estimated from the ALOG growth curve of Tanaka (1982). In a second case, a simulation approach was used that required that a set of 20 individuals meet four criteria in comparison with the observed set, a mean age close to that observed, a variance in age close to that observed, a mean age differential between pairs of individuals ordered by age close to that observed, and a mean variance in the age differential close to that observed.

In the case of estimating ages from the ALOG growth curve, the ages predicted do not align with those produced by the observed age frequency. This is due to the high variability in size at age (Fig. 2), especially for the older animals, so this method cannot be used to predict the population age frequency of ocean quahogs. The simulation approach produced a distribution similar to the age frequency that is produced from only the

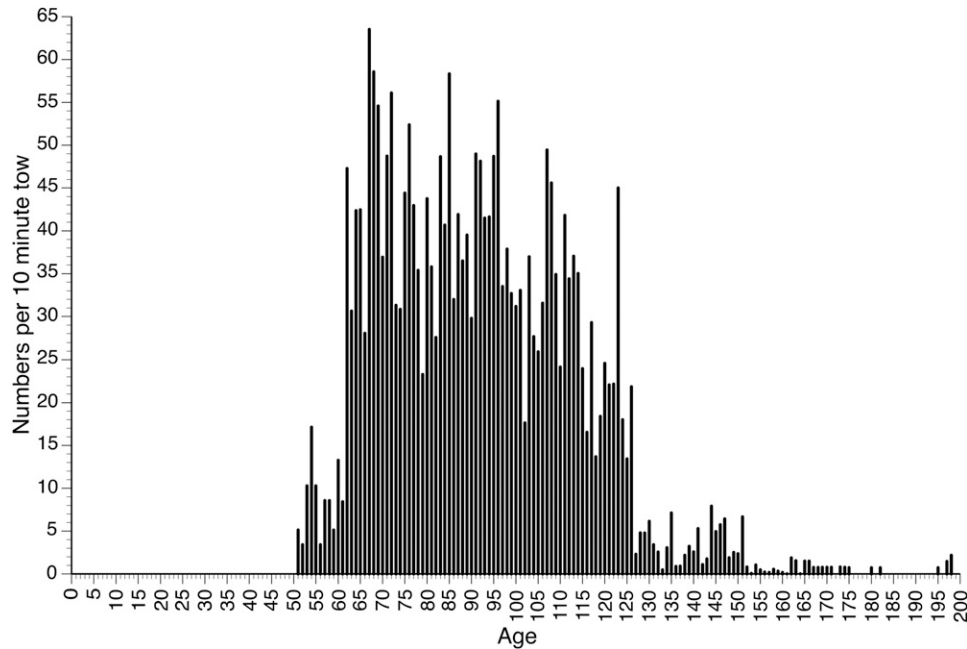


Figure 6. Age–frequency distribution of the Georges Bank population.

observed ages. The simulation approach distributes individuals in the observed age frequency to ages that were absent due to the low sample size. A direct test of the assumption that many ages likely to be present were not observed demonstrated the verity of this expectation (Table 3). Thus, the simulation approach likely provides a more realistic age distribution among all ages within the observed age range.

Age Frequency of a Georges Bank Population: Implications

As the last surviving member of the family Arctiidae, ocean quahogs have inhabited areas along the continental shelf of the North Atlantic Basin and adjacent European seas since the Late Mesozoic (Morton 2011). Considering that these animals have been present along the boreal North Atlantic shelf for such an extended period of time, it is perhaps surprising to find animals no older than about 200 y on Georges Bank, suggesting colonization sometime very early in the 1800s. One possible hypothesis is that the establishment of the ocean quahog population on this portion of Georges Bank co-occurred with the ending of the Little Ice Age, which is thought to have ended sometime in the early to mid-19th century (for more on the Little Ice Age, see Schöne et al. 2005b, Mann et al. 2009, Cronin et al. 2010). During the Little Ice Age, bottom water temperatures would have been much colder on Georges Bank than observed today. As the end of the Little Ice Age approached, warming waters would have permitted movement of the ocean quahog population into the region of Georges Bank sampled for this study. Recent examination of the distribution of ocean quahog shells on Georges Bank lends credence to this scenario as shells, but no live animals, are found at shallower depths on the bank today (Powell et al., unpublished data), in a region that arguably would have had more appropriate bottom water temperatures for ocean quahogs in earlier times.

Regardless, once the initial recruits were established where ocean quahogs now live on Georges Bank, the population

remained at low levels for about 70 y, evident from the long tail in the population age frequency (Fig. 6). Taking the analogy of a species invasion for this colonization event, time lags after initial colonization are not uncommon (Diederich et al. 2005, Facon & David 2006, Karatayev et al. 2011). The time lag from a small population size until the propagation of the population is likely a result of delayed maturity in ocean quahogs. As ocean quahogs do not reach maturity for several decades following settlement, the population perforce would have to remain small in size for many years, unless recruitment from outside the region increased. Evidence suggests that it did not. Of course, one cannot discount the possibility that the occupation remained limited because the environment remained suboptimal until the late 1800s.

The rapid expansion of the population late in the 1800s suggests that one of several events occurred. Once enough animals reached maturity, a local Allee effect might have been overcome, permitting much enhanced recruitment. Fertilization efficiency can be expected to be poor in sparse populations of relatively immobile molluscs (Shepherd et al. 1998, Hodgson et al. 2007, Luttikhuisen et al. 2011). Alternatively, increased water temperatures or a change in food supply might have permitted increased spawning and enhanced survivorship to maturity (Hofmann et al. 1992, Munroe et al. 2013, Svensson & Marshall 2015). Less likely, perhaps, but still possible given the extended larval life span (Lutz et al. 1982), increased recruitment from outside the region may have occurred. The latter is not consistent with the limited larval connectivity of Georges Bank with external regions observed today (Zhang et al. 2015), but such connectivity may not have been required if ocean quahogs occupied a shallower portion of the bank in the 1800s.

Once the population expansion occurred in the late 1800s, the population rapidly approached an asymptote and stabilized, suggesting that the population probably reached carrying capacity. This is supported in the literature, as ocean quahog

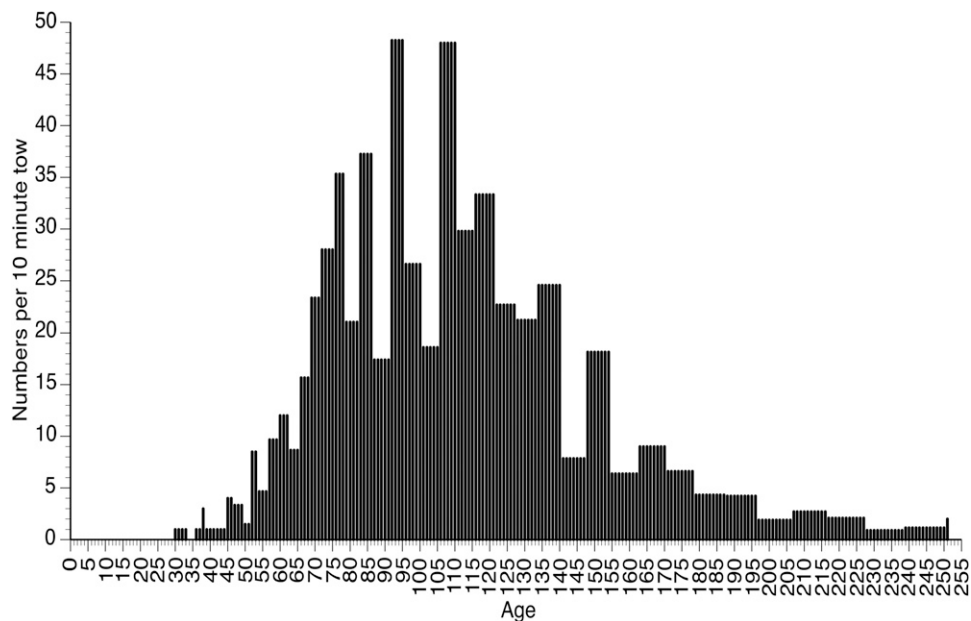


Figure 7. Age–frequency distribution generated from the Tanaka growth curve.

populations in the mid-Atlantic were considered to be at carrying capacity prior to the beginning of the fishery in the late 1960s (NESFC 2009) and the stock on Georges Bank effectively has never been fished. The rapid population expansion, then, encompassing about 30 y, is not inconsistent with molluscan population dynamics (Carlton et al. 1990, Zolotarev 1996, Brandt et al. 2008), but is surprising given the population dynamics of many long-lived species, and perhaps counterintuitive with the lower metabolic rate of this species in comparison with other bivalves (Begum et al. 2009, Ungvari et al. 2013). As the population stabilized early in the 1900s, recruitment was essentially continuous, though low enough to balance mortality. Currently, the ocean quahog stock is considered to be relatively unproductive, with literature suggesting that the recruitment rate is low and infrequent (Powell & Mann 2005). This type of recruitment is characteristic of a stock that is expected to be near carrying capacity, wherein recruitment is in balance with the low mortality rate characteristic of a long-lived species. Nonetheless, the record of colonization on Georges Bank suggests that the species is a capable and rapid invader once environmental conditions are met and once the initial restriction on spawning success produced by low population density and slow growth to maturity is overcome.

The age–frequency distribution bears many similarities to the one presented by Ridgway et al. (2012) for the Belfast Lough, Northern Ireland, and by Steingrímsson and Thórarinsdóttir (1995) for Iceland. Both Ridgway et al. (2012) and Steingrímsson and Thórarinsdóttir (1995) observe an approximately 100-y

period of low abundance beginning about 200–220 y BP, followed by a rapid rise in numbers at age over an approximately 20-y period. The subsequent record also asymptotes at what might be interpreted as carrying capacity. Ridgway et al. (2012) record only minor breaks in what is a generally consistent recruitment record over the time span represented by the age frequency, also similar to our results. Steingrímsson and Thórarinsdóttir (1995) document less consistent recruitment with what might be considered broad age classes, although the overall pattern of recruitment as determined from abundance at age remains similar. Whether this type of colonization record is typical of ocean quahogs is unclear, but the similarity between the three sites, well separated in space, poses an interesting possibility.

ACKNOWLEDGMENTS

We appreciate the assistance of the Captain and crew of the *F/V Pursuit*, who carried out these sampling tasks at sea. This research was supported by the National Science Foundation Industry/University Cooperative Research Center SCeMFIS (Science Center for Marine Fisheries) through membership fees under the direction of the Industry Advisory Board (IAB). SCeMFIS administrative support is provided by NSF award no. 1266057. Conclusions and opinions expressed herein are solely those of the authors. We also thank Melissa Southworth (VIMS) who assisted in the cumbersome task of sample sorting.

LITERATURE CITED

- Appleyard, C. L. & J. T. DeAlteris. 2001. Modeling growth of the northern quahog, *Mercenaria mercenaria*. *J. Shellfish Res.* 20:1117–1125.
- Begum, S., L. Basova, J. Strahl, A. Sakhotin, O. Heilmayer, E. Philipp, T. Brey & D. Abele. 2009. A metabolic model for the ocean quahog *Arctica islandica*—Effects of animal mass and age, temperature, salinity, and geography on respiration rate. *J. Shellfish Res.* 28:533–539.
- Begum, S., L. Basova, O. Heilmayer, E. E. R. Philipp, D. Abele & T. Brey. 2010. Growth and energy budget models of the bivalve *Arctica*

- islandica* at six different sites in the northeast Atlantic realm. *J. Shellfish Res.* 29:107–115.
- Boukal, D. S., U. Dieckmann, K. Enberg, M. Heino & C. Jørgensen. 2014. Life-history implications of the allometric scaling of growth. *J. Theor. Biol.* 359:199–207.
- Brey, T., W. E. Arntz, D. Pauly & H. Rumohr. 1990. *Arctica* (*Cyprina*) *islandica* in Kiel Bay (western Baltic): growth, production and ecological significance. *J. Exp. Mar. Biol. Ecol.* 136:217–235.
- Brandt, G., A. Wehrmann & K. W. Wirtz. 2008. Rapid invasion of *Crassostrea gigas* into the German Wadden Sea dominated by larval supply. *J. Sea Res.* 59:279–296.
- Butler, P. G., C. A. Richardson, J. D. Scourse, R. Witbaard, B. R. Schöne, N. M. Fraser, A. D. Wanamaker, Jr., C. L. Bryant, I. Harris & I. Robertson. 2009. Accurate increment identification and the spatial extent of the common signal in five *Arctica islandica* chronologies from the Fladen Ground, northern North Sea. *Paleoceanography* 24:1–18.
- Butler, P. G., A. D. Wanamaker, Jr., J. D. Scourse, C. A. Richardson & D. J. Reynolds. 2013. Variability of marine climate on the North Icelandic Shelf in a 1357-year proxy archive based on growth increments in the bivalve *Arctica islandica*. *Palaeogeogr. Palaeoclimatol. Palaeoecol.* 373:141–151.
- Butterworth, K. G., M. K. Grieshaber & A. C. Taylor. 2004. Sulphide detoxification in the bivalve, *Arctica islandica* (L.) from two different habitats. *Ophelia* 58:101–113.
- Cargnelli, L. M., S. J. Griesbach, D. B. Packer & E. Weissberger. 1999a. Essential fish habitat source document: ocean quahog, *Arctica islandica*, life history and habitat characteristics. NOAA Technical Memorandum NMFS-NE-148. Woods Hole, MA: U.S. Department of Commerce. 12 pp.
- Cargnelli, L. M., S. J. Griesbach, D. B. Packer & E. Weissberger. 1999b. Essential fish habitat source document: Atlantic surfclam, *Spisula solidissima*, life history and habitat characteristics. NOAA Technical Memorandum NMFS-NE-142. Woods Hole, MA: U.S. Department of Commerce. 13 pp.
- Carlton, J. T., J. K. Thompson, L. E. Schemel & F. H. Nichols. 1990. Remarkable invasion of San Francisco Bay (California, USA) by the Asian clam, *Potamocorbula amurensis* I. Introduction and dispersal. *Mar. Ecol. Prog. Ser.* 66:81–94.
- Chintala, M. M. & J. P. Grassle. 2001. Comparison of recruitment frequency and growth of surfclams, *Spisula solidissima* (Dillwyn, 1817), in different inner-shelf habitats of New Jersey. *J. Shellfish Res.* 20:1177–1186.
- Cronin, T. M., K. Hayo, R. C. Thunell, G. S. Dwyer, C. Saenger & D. A. Willard. 2010. The medieval climate anomaly and little ice age in Chesapeake Bay and the north Atlantic Ocean. *Palaeogeogr. Palaeoclimatol. Palaeoecol.* 297:299–310.
- Dahlgren, T. G., J. R. Weinberg & K. M. Halanych. 2000. Phylogeography of the ocean quahog (*Arctica islandica*): influences of paleoclimate on genetic diversity and species range. *Mar. Biol.* 137:487–495.
- Diederich, S., G. Nehls, J. E. E. van Beusekom & K. Reise. 2005. Introduced Pacific oysters (*Crassostrea gigas*) in the northern Wadden Sea: invasion accelerated by warm summers? *Helgol. Mar. Res.* 59:97–106.
- Ebert, T. A., J. D. Dixon, S. C. Schroeter, P. E. Kalvass, N. T. Richmond, W. A. Bradbury & D. A. Woodby. 1999. Growth and mortality of red sea urchins *Strongylocentrotus franciscanus* across a latitudinal gradient. *Mar. Ecol. Prog. Ser.* 190:189–209.
- Ebert, T. A. & J. R. Southon. 2003. Red sea urchins (*Strongylocentrotus franciscanus*) can live over 100 years: confirmation with A-bomb ¹⁴carbon. *Fish Bull.* 101:915–922.
- Facon, B. & P. David. 2006. Metapopulation dynamics and biological invasions: a spatially explicit model applied to a freshwater snail. *Am. Nat.* 168:769–783.
- Flores, L., B. Ernst & A. M. Parma. 2010. Growth pattern of the sea urchin, *Loxechinus albus* (Molina, 1782) in southern Chile: evaluation of growth models. *Mar. Biol.* 157:967–977.
- Foster, L. C., A. A. Finch, N. A. Finch & C. Andersson. 2009. Strontium distribution in the shell of the aragonite bivalve *Arctica islandica*. *Geochim. Geophys. Geosyst.* 10:1–14.
- Gilkinson, K. D., D. C. Gordon, Jr., K. G. MacIsaac, D. L. McKeown, E. C. R. Kenchington, C. Bourbonnais & W. P. Voss. 2005. Immediate impacts and recovery trajectories of macrofaunal communities following hydraulic clam dredging on Banquereau, eastern Canada. *ICES J. Mar. Sci.* 62:925–947.
- Harding, J. M., S. E. King, E. N. Powell & R. Mann. 2008. Decadal trends in age structure and recruitment patterns of ocean quahogs, *Arctica islandica* from the Mid-Atlantic Bight in relation to water temperature. *J. Shellfish Res.* 27:667–690.
- Hennen, D. R. 2015. How should we harvest an animal that can live for centuries? *N. Am. J. Fish. Manage.* 35:512–527.
- Hodgson, A. N., W. J. F. le Quesne, S. J. Hawkins & J. D. Bishop. 2007. Factors affecting fertilization success in two species of patellid limpet (Mollusca: Gastropoda) and development of fertilization kinetics models. *Mar. Biol.* 150:415–426.
- Hofmann, E. E., E. N. Powell, J. M. Klinck & E. A. Wilson. 1992. Modeling oyster populations. III. Critical feeding periods, growth and reproduction. *J. Shellfish Res.* 11:399–416.
- Jones, D. S. 1980. Annual cycle of shell growth increment formation in two continental shelf bivalves and its paleoecologic significance. *Paleobiology* 6:331–340.
- Karatayev, A. Y., L. E. Burlakova, S. E. Mastitsky & D. K. Padilla. 2011. Contrasting rates of spread of two congeners, *Dreissena polymorpha* and *Dreissena rostriformis bugensis*, at different spatial scales. *J. Shellfish Res.* 30:923–931.
- Karkach, A. S. 2006. Trajectories and models of individual growth. *Demogr. Res.* 15:347–400.
- Kimura, D. K. & S. Chikani. 1987. Mixtures of empirical distributions: an iterative application of the age-length key. *Biometrics* 43:23–35.
- Lewis, C. V. W., J. R. Weinberg & C. S. Davis. 2001. Population structure and recruitment of the bivalve *Arctica islandica* (Linnaeus, 1767) on Georges Bank from 1980–1999. *J. Shellfish Res.* 20:1135–1144.
- Luttikhuisen, P. C., P. J. C. Honkoop & J. Drent. 2011. Intraspecific egg size variation and sperm limitation in the broadcast spawning bivalve *Macoma balthica*. *J. Exp. Mar. Biol. Ecol.* 396:156–161.
- Lutz, R. A., R. Mann, J. G. Goodsell & M. Castagna. 1982. Larval and early post-larval development of *Arctica islandica*. *J. Mar. Biol. Ass. U.K.* 62:745–769.
- Mann, M. E., Z. Zhang, S. Rutherford, R. S. Bradley, M. K. Hughes, D. Shindell, C. Ammann, G. F. Foluwegi & F. Ni. 2009. Global signatures and dynamical origins of the Little Ice Age and Medieval Climate Anomaly. *Science* 326:1256–1260.
- McCuaig, J. M. & R. H. Green. 1983. Unionid growth curves derived from annual rings: a baseline model for Long Point Bay, Lake Erie. *Can. J. Fish. Aquat. Sci.* 40:436–442.
- Merrill, A. S. & J. W. Ropes. 1969. The general distribution of the surf clam and ocean quahog. *Proc. Natl. Shellfish. Assoc.* 59:40–45.
- Morton, B. 2011. The biology and functional morphology of *Arctica islandica* (Bivalvia: Arctiidae): a gerontophilic living fossil. *Mar. Biol. Res.* 7:540–553.
- Munroe, D. M., E. N. Powell, R. Mann, J. M. Klinck & E. E. Hofmann. 2013. Underestimation of primary productivity on continental shelves: evidence from maximum size of extant surfclam (*Spisula solidissima*) populations. *Fish. Oceanogr.* 22:220–233.
- Murawski, S. A., J. W. Ropes & F. M. Serchuk. 1982. Growth of the ocean quahog, *Arctica islandica*, in the Mid-Atlantic Bight. *Fish Bull.* 80:21–34.
- NEFSC. 2009. 48th Northeast Regional Stock Assessment Workshop (48th SAW) assessment report. NEFSC Reference Document 09-15. Woods Hole, MA: U.S. Department of Commerce. 834 pp.
- Noreen, E. W. 1989. Computer-intensive methods for testing hypotheses: an introduction. New York, NY: John Wiley & Sons. 229 pp.

- Oeschger, R. 1990. Long-term anaerobiosis in sublittoral marine invertebrates from the western Baltic Sea: *Halicryptus spinulosus* (Priapulida), *Astarte borealis* and *Arctica islandica* (Bivalvia). *Mar. Ecol. Prog. Ser.* 59:133–143.
- Philipp, E. E. R. & D. Abele. 2010. Masters of longevity: lessons from long-lived bivalves—a mini-review. *Gerontology* 56:55–65.
- Powell, E. N. & R. Mann. 2005. Evidence of recent recruitment in the ocean quahog *Arctica islandica* in the Mid-Atlantic Bight. *J. Shellfish Res.* 24:517–530.
- Ragnarsson, S. A. & G. G. Thórarinsdóttir. 2002. Abundance of ocean quahog, *Arctica islandica*, assessed by underwater photography and a hydraulic dredge. *J. Shellfish Res.* 21:673–676.
- Ridgway, I. D. & C. A. Richardson. 2011. *Arctica islandica*: the longest lived non colonial animal known to science. *Rev. Fish Biol. Fish.* 21:297–310.
- Ridgway, I. D., C. A. Richardson, J. D. Scourse, P. G. Butler & D. J. Reynolds. 2012. The population structure and biology of the ocean quahog, *Arctica islandica*, in Belfast Lough, northern Ireland. *J. Mar. Biol. Ass. U.K.* 92:539–546.
- Rogers-Bennett, L., D. W. Rogers & S. A. Schultz. 2007. Modeling growth and mortality of red abalone (*Haliotis rufescens*) in northern California. *J. Shellfish Res.* 26:719–727.
- Ropes, J. W., D. S. Jones, S. A. Murawski, F. M. Serchuk & A. Jearld, Jr. 1984. Documentation of annual growth lines in ocean quahogs, *Arctica islandica* Linné. *Fish Bull.* 82:1–19.
- Rowell, T. W., D. R. Chaisson & J. T. McLane. 1990. Size and age of sexual maturity and annual gametogenic cycle in the ocean quahog, *Arctica islandica* (Linnaeus, 1767), from coastal waters in Nova Scotia, Canada. *J. Shellfish Res.* 9:195–203.
- Sager, G. & R. Sammler. 1983. Mathematical investigations into the longevity of the ocean quahog *Arctica islandica* (Mollusca: Bivalvia). *Int. Rev. Gesamten Hydrobiol.* 68:113–120.
- Schöne, B. R., J. Fiebig, M. Pfeiffer, R. Gleß, J. Hickson, A. L. A. Johnson, W. Dreyer & W. Oschmann. 2005a. Climate records from a bivalved Methuselah (*Arctica islandica*, Mollusca; Iceland). *Palaeogeogr. Palaeoclimatol. Palaeoecol.* 212:215–232.
- Schöne, B. R., M. Pfeiffer, T. Pohlmann & F. Seigismund. 2005b. A seasonally resolved bottom-water temperature record for the period AD 1866–2002 based on shells of *Arctica islandica* (Mollusca; North Sea). *Int. J. Climatol.* 25:947–962.
- Schöne, B. R. 2013. *Arctica islandica* (Bivalvia): a unique paleoenvironmental archive of the northern North Atlantic Ocean. *Global Planet. Change* 111:199–225.
- Shepherd, S. A., J. R. Turrubiates-Morales & K. Hall. 1998. Decline of the abalone fishery at La Natividad, México: overfishing or climate change. *J. Shellfish Res.* 17:839–846.
- Solidoro, C., R. Pastres, D. M. Canu, M. Pellizzato & R. Rossi. 2000. Modelling the growth of *Tapes philippinarum* in northern Adriatic lagoons. *Mar. Ecol. Prog. Ser.* 199:137–148.
- Stari, T., K. F. Preedy, E. McKenzie, W. S. C. Gurney, M. R. Heuth, P. A. Kunzlik & D. C. Speirs. 2010. Smooth age length keys: observations and implications for data collection on North Sea haddock. *Fish. Res.* 105:2–12.
- Steingrímsson, S. A. & G. Thórarinsdóttir. 1995. Age structure, growth and size at sexual maturity in ocean quahog, *Arctica islandica* (Mollusca: Bivalvia), off NW-Iceland. ICES document C.M. 1995/K, vol. 54. Reykjavik, Iceland: Marine Research Institute. 17 pp.
- Svensson, J. R. & D. J. Marshall. 2015. Limiting resources in sessile systems: food enhances diversity and growth of suspension feeders despite available space. *Ecology* 96:819–827.
- Tanaka, M. 1982. A new growth curve which expresses infinitive increase. *Amakusa Mar. Biol. Lab* 6:167–177.
- Tanaka, M. 1988. Eco-physiological meaning of parameters of ALOG growth curve. *Amakusa Mar. Biol. Lab* 9:103–106.
- Taylor, A. C. 1976. Burrowing behavior and anaerobiosis in the bivalve *Arctica islandica* (L.). *J. Mar. Biol. Ass. U.K.* 56:95–109.
- Taylor, A. C. & A. B. Brand. 1975. Effects of hypoxia and body size on the oxygen consumption of the bivalve *Arctica islandica* (L.). *J. Exp. Mar. Biol. Ecol.* 19:187–196.
- Thórarinsdóttir, G. G. & L. D. Jacobson. 2005. Fishery biology and biological reference points for management of ocean quahogs (*Arctica islandica*) off Iceland. *Fish. Res.* 75:97–106.
- Thórarinsdóttir, G. G. & S. A. Steingrímsson. 2000. Size and age at sexual maturity and sex ratio in ocean quahog, *Arctica islandica* (Linnaeus, 1767), off northwest Iceland. *J. Shellfish Res.* 19:943–947.
- Titschack, J., M. Zuschin, C. Spötl & C. Baal. 2010. The giant oyster *Hyothis hyotis* from the northern Red Sea as a decadal-scale archive for seasonal environmental fluctuations in coral reef habitats. *Coral Reefs* 29:1061–1075.
- Ungvari, Z., D. Sosnowska, J. B. Mason, H. Gruber, S. W. Lee, T. S. Schwartz, M. K. Brown, N. J. Storm, K. Fortney, J. Sowa, A. B. Byrne, T. Kurz, E. Levy, W. E. Sonntag, S. N. Austad, A. Csizsar & J. Ridgway. 2013. Resistance to genotoxic stresses in *Arctica islandica*, the longest living noncolonial animal: is extreme longevity associated with a multistress resistance phenotype? *J. Gerontol. A Biol. Sci. Med. Sci.* 68:521–529.
- Urban, H. J. 2002. Modeling growth of different developmental stages in bivalves. *Mar. Ecol. Prog. Ser.* 238:109–114.
- Wanamaker, A. D., Jr., J. Heinemeier, J. D. Scourse, C. A. Richardson, P. G. Butler, J. Eriksson & K. L. Knudsen. 2008. Very long-lived mollusks confirm 17th century AD tephra-based radiocarbon reservoir ages for North Icelandic shelf waters. *Radiocarbon* 50:399–412.
- Weinberg, J. R. 2005. Bathymetric shift in the distribution of Atlantic surfclams: response to warmer ocean. *ICES J. Mar. Sci.* 62:1444–1453.
- Winter, J. 1978. Filter feeding and food utilization in *Arctica islandica* L. and *Modiolus modiolus* L. at different food concentrations. In: Steel, J. H., editor. Marine food chains. Edinburgh, Scotland: Oliver and Boyd. pp. 196–206.
- Wisshak, M., M. L. Correa, S. Gofas, C. Salas, M. Taviani, J. Jakobsen & A. Freiwald. 2009. Shell architecture, element composition, and stable isotope signature of the giant deep-sea oyster, *Neopycnodonte zibrowii* sp. n. from the NE Atlantic. *Deep Sea Res. Part I Oceanogr. Res. Pap.* 56:374–407.
- Witbaard, R. & M. J. N. Bergman. 2003. The distribution and population structure of the bivalve *Arctica islandica* L. in the North Sea: what possible factors are involved? *J. Sea Res.* 50:11–25.
- Zhang, X., D. Haidvogel, D. Munroe, E. N. Powell, J. Klinck, R. Mann & F. S. Castruccio. 2015. Modeling larval connectivity of the Atlantic surfclams within the Middle Atlantic Bight: model development, larval dispersal and metapopulation connectivity. *Estuar. Coast. Shelf Sci.* 153:38–53.
- Zolotarev, V. 1996. The Black Sea ecosystem changes related to the introduction of new mollusc species. *P.S.Z.N.I: Mar. Ecol.* 17:227–236.